

# Theoretical Study of the Transition Energies of the Visible Absorption Spectra of $[\text{RhCl}_6]^{3-}$ and $[\text{RhCl}_5(\text{H}_2\text{O})]^{2-}$ Complexes in Aqueous Solution

Kazunaka Endo,\* Masahiko Saikawa,† Manabu Sugimoto,††

Masahiko Hada,†† and Hiroshi Nakatsuji††

Tsukuba Research Laboratory, Mitsubishi Paper Mills, Ltd., 46 Wadai, Tsukuba, Ibaraki 300-42

†R&D Laboratory for Photo Materials, Mitsubishi Paper Mills, Ltd., Nagaokakyo, Kyoto 617

††Department of Synthetic Chemistry and Biological Chemistry, Faculty of Engineering, Kyoto University, Yoshida-honmachi, Sakyo-ku, Kyoto 606

(Received October 17, 1994)

Electron absorption spectra of  $[\text{RhCl}_6]^{3-}$  and  $[\text{RhCl}_5(\text{H}_2\text{O})]^{2-}$  complexes are studied theoretically by the ab initio symmetry adapted cluster (SAC)/SAC-CI method. Two maximum peaks of the visible absorption spectra in the range of 300—600 nm observed in aqueous solution are assigned to ( $^1\text{T}_{1g}$ ;  $^1\text{T}_{2g}$ ) and mixing- ( $1\text{B}_1$ ,  $1\text{A}_2$ ,  $1\text{B}_2$ ;  $2\text{B}_1$ ,  $2\text{A}_2$ ,  $2\text{B}_2$ ) states for  $[\text{RhCl}_6]^{3-}$  and  $[\text{RhCl}_5(\text{H}_2\text{O})]^{2-}$  complexes, respectively, in good agreement. These states are due to the forbidden d-d transitions from the  $\text{Rh}(d\pi) + \text{Ligand}(p\pi)$  bonding MOs to the  $\text{Rh}(d\sigma) - \text{Ligand}(p\sigma)$  antibonding MOs, leading to an weakening of the metal-ligand bonds.

The  $[\text{RhCl}_n(\text{H}_2\text{O})_{6-n}]^{(n-3)-}$  species are typical of octahedral transition metal compounds and are important as doping agents for manufacturing AgX photographic emulsions; they affect the sensitivity and the gradation of AgX emulsions. There are two papers<sup>1,2)</sup> that discuss the effects of  $[\text{RhX}_{6-n}(\text{H}_2\text{O})_n]^{n-3}$  ( $n=0, 1, 2$ ) complexes on the sensitivity of the AgX photoemulsions. We have shown that the relative sensitivity of cubic AgCl and AgBr emulsions increases by about 2—3 times as the  $\text{H}_2\text{O}$  coordination number in  $[\text{RhX}_{6-n}(\text{H}_2\text{O})_n]^{n-3}$  ( $n=0, 1, 2$ ) increased in comparison with the standard AgX emulsion containing  $[\text{RhX}_6]^{3-}$ .<sup>2)</sup> When rhodium complexes are added, the AgX emulsions are usually stabilized in an aqueous halogenide ion solution as observed by visible absorption spectrum measurements. The AgX emulsions are made by the controlled double-jet addition of  $\text{AgNO}_3$  and  $\text{X}^-$  ( $\text{NaCl}$ ,  $\text{KBr}$  for  $\text{X}=\text{Cl}$ ,  $\text{Br}$ ; respectively) solutions containing  $[\text{RhX}_{6-n}(\text{H}_2\text{O})_n]^{n-3}$  ( $n=0, 1, 2$ ) complexes at a constant rate to an aqueous solution of inert bone gelatin. The molar ratio for rhodium(III)-complex/ $\text{NaCl}$ (or  $\text{KBr}$ ) is adjusted to  $2.0 \times 10^{-6}$  to 1.

Several experimental studies<sup>3-7)</sup> have been reported on the kinetics of the  $[\text{RhCl}_n(\text{H}_2\text{O})_{6-n}]^{(n-3)-}$  system in acidic aqueous solution. These species are of further interest as potential catalysts for reactions such as the oxidation of ethylene to acetaldehyde.<sup>8)</sup> Finally, a kinetic study<sup>6)</sup> of the steric course of the entire series of aquation-anation reactions of the Rh(III) chloroqua complexes demonstrated that they are controlled by the

trans effect of the chloride ligands involving an unsymmetrical, five-coordinate intermediate, probably in the form of a square pyramid.

These experimental studies focused on the kinetic and spectroscopic results, and so the investigators assigned the peaks in the visible spectrum to the Rh(III) complexes, as transitions from the  $^1\text{A}_{1g}$  ground state to the  $^1\text{T}_{1g}$  and  $^1\text{T}_{2g}$  upper states, just as in the energy diagram for Fe(II) and Co(III) by the ligand field theory. The splitting value,  $Qq$ , in the ligand field absorption band was estimated from the observed spectra.

We here attempt to characterize the first and second peaks in the absorption spectra of the  $[\text{RhCl}_6]^{3-}$  and  $[\text{RhCl}_5(\text{H}_2\text{O})]^{2-}$  complexes in aqueous solutions using a reliable, ab initio theoretical method, which includes sufficient electron correlations. We use the ab initio symmetry adapted cluster expansion (SAC)<sup>9)</sup> method and the SAC-CI method,<sup>10)</sup> which have been applied to a number of molecules including transition metal complexes.<sup>11,12)</sup> This method has been shown to be useful for investigating the spectroscopies of excited and ionized states of molecules and has yielded many reliable new assignments of the experimental spectra. We will finally describe briefly the mechanism of the desensitization produced by adding Rh(III) chloroqua complexes to the AgCl grain in the emulsion.

## Calculational Method

The energy and the electronic structure of the rhodium complexes are calculated by the SAC method

for the ground state and by the SAC-CI method for the excited states. The SAC expansion is an accurate method for describing the dynamic correlation in the ground state. The SAC-CI expansion is more rapidly convergent than an ordinary CI expansion because it is based on the excited functions that satisfy the necessary conditions for the excited states, and because it starts from the ground-state correlation. The SAC/SAC-CI method has been established as reliable for calculating ground, excited and ionized states. For more details, see the review article given in the reference.<sup>12)</sup>

The gaussian basis set for the Rh was the (111/21/211) valence orbital, that for Cl was the (21/21) valence orbital, and the inner cores were replaced by the effective core potentials.<sup>13,14)</sup> We used the [4s2p] set for oxygen and the [2s] set<sup>15)</sup> for hydrogen. The symmetries of the complexes  $[\text{RhCl}_6]^{3-}$  and  $[\text{RhCl}_5(\text{H}_2\text{O})]^{2-}$  are  $O_h$  and  $C_{2v}$ , respectively. The bond lengths for the Rh complexes are 2.50 Å for Rh-Cl; 2.06 Å for Rh-O and 0.958 Å for O-H of water. The angle of water is 104.45°. The Hartree-Fock MOs calculated by the GAMESS program<sup>16)</sup> were used as the reference orbitals. In the SAC/SAC-CI calculations, we included all single excitations and selected double excitations in the linked terms. The unlinked terms consist of the product of the double excitations in the SAC calculations and of the product of the single and double excitations in the SAC-CI calculations.

### Experimental

The electronic spectra of the rhodium complexes were measured with a Shimadzu UV-3100S spectrometer at room temperature (25 °C). The measurements were done in a day, after the  $[\text{RhCl}_6]^{3-}$  and  $[\text{RhCl}_5(\text{H}_2\text{O})]^{2-}$  complexes had been prepared. The observed spectra were in good accordance with the earlier studies.<sup>3,4)</sup>

### Results and Discussion

#### A. The Ground States of the Rh(III) Complexes.

The rhodium chloroaqua complexes are known to have a diamagnetic ground state. Tables 1 and 2 show the energies and nature of the Hartree-Fock orbitals for the ground states of  $[\text{RhCl}_6]^{3-}$  and  $[\text{RhCl}_5(\text{H}_2\text{O})]^{2-}$ , respectively.

In Table 1 for  $[\text{RhCl}_6]^{3-}$ , the lowest occupied MOs are the threefold degenerate  $1t_{2g}$  MOs, which are  $\pi$  bonding between the Rh and Cl atoms. It is composed of (Rh  $d_{xy}$ -Cl  $p_x$ ,  $p_y$ ), (Rh  $d_{xz}$ -Cl  $p_x$ ,  $p_z$ ), and (Rh  $d_{yz}$ -Cl  $p_y$ ,  $p_z$ ) pairs. The next occupied  $1a_{1g}$  MO is an essentially localized 5s AO of Rh and the next  $1e_g$  MOs are  $\sigma$ -bonding between the Rh and Cl atoms. The next two occupied MOs, threefold degenerate  $1t_{1u}$ , and  $2t_{2g}$  MOs, are  $\sigma$ -bonding and  $\pi$ -bonding MOs between the Rh and Cl atoms. Among the three highest occupied MOs,  $2t_{1u}$  and  $4t_{1u}$  MOs are nonbonding long-pair orbitals localized on the ligands, and  $3t_{1u}$  MOs are  $\pi$ -bonding between the Rh p and Cl p orbitals.

The lowest unoccupied MOs is the twofold degenerate  $2e_g$  MOs, which are  $\sigma$ -antibonding between the Rh d

and Cl p orbitals. The next  $5t_{1u}$  MOs are  $\pi$ -antibonding between Rh p and Cl p MOs. The next  $2a_{1g}$  MO is the  $\sigma$ -antibonding orbital. These orbitals are important for understanding the primary nature of the excitations in the  $[\text{RhCl}_6]^{3-}$  complex.

We give similar information on the Hartree-Fock MO's of  $[\text{RhCl}_5(\text{H}_2\text{O})]^{2-}$  in Table 2. Note that the orbital energies are shifted lower for the difference in the formal charge and that the symmetry here is  $C_{2v}$ .

Table 3 shows the Hartree-Fock, SAC, and correlation energies for the ground state of the rhodium chloroaqua complexes. The correlation energy is the difference between the SAC and the Hartree-Fock energies. The electron correlation works to relax the ionicity overestimation in the Hartree-Fock level.

**B. The Transition Energies of the Excited States for the Rh(III) Complexes.** The two excitations of the Rh(III) complexes in the visible region had been assigned as the transitions from the  $^1A_{1g}$  to the  $^1T_{1g}$  and  $^1T_{2g}$  states by the simple Huckel method using the ligand field theory.<sup>17)</sup> We give here more exact assignment of the transitions in the absorption spectra of the Rh(III) complexes using a reliable ab initio SAC/SAC CI theories.

Table 4 shows the main configurations of the excited states and the calculated transition energies compared with the values observed in aqueous solutions.<sup>7,18)</sup> The two excitations are assigned as the transitions to the ( $^1T_{1g}$ ;  $^1T_{2g}$ ) and the mixed ( $1B_1$ ,  $1A_2$ ,  $1B_2$ ;  $2B_1$ ,  $2A_2$ ,  $2B_2$ ) states for  $[\text{RhCl}_6]^{3-}$  and  $[\text{RhCl}_5(\text{H}_2\text{O})]^{2-}$  complexes, respectively, by the SAC-CI method. The calculated transition energies are in good accordance with the experimental ones (see Fig. 1).

The  $^1T_{1g}$  and  $^1T_{2g}$  excitations of the  $[\text{RhCl}_6]^{3-}$  complex are due to  $t_{2g}$ -to- $e_g$  transitions from the analysis of the SAC-CI result. These transitions correspond to the forbidden d-d transitions. In more detail, the main configuration of the  $^1T_{1g}$  state corresponds to the  $2t_{2g}$ -to- $2e_g$  transition from Rh( $d\pi$ )+Cl( $p\pi$ ) bonding MOs to Rh( $d\sigma$ )+Cl( $p\sigma$ ) antibonding MOs (Table 1). The small contribution comes from the  $1t_{2g}$ -to- $2e_g$  excitations. For the  $^1T_{2g}$  state, the relative contribution of the two  $t_{2g}$ -to- $e_g$  transitions is reversed as shown in Table 4.

For the  $C_{2v}$   $[\text{RhCl}_5(\text{H}_2\text{O})]^{2-}$  complex, the mixed ( $1B_1$ ,  $1A_2$ ,  $1B_2$ ) and ( $2B_1$ ,  $2A_2$ ,  $2B_2$ ) transitions result from the ( $a_2$ ,  $b_1$ ,  $b_2$ )-to- $a_1$  excitations, which are again due to the d-to-d transitions from the three Rh-( $d\pi$ )+Cl( $p\pi$ ), or O( $p\pi$ ) bonding MOs to the two Rh-( $d\sigma$ )-Cl( $p\sigma$ ), or O( $p\sigma$ ) antibonding MOs (see Tables 2 and 4). These transitions correspond to the  $t_{2g}$ -to- $e_g$  excitations in the octahedral  $[\text{RhCl}_6]^{3-}$  complex.

In these Rh-complexes, we can see degenerate or pseudo-degenerate effects of the excited states like those in most metalcomplexes using the SAC/SAC CI method. For  $[\text{RhCl}_6]^{3-}$  complex, the excited state has complete degenerate, while, in the case of  $[\text{RhCl}_5(\text{H}_2\text{O})]^{2-}$ , we gave some closely degenerate re-

Table 1. Orbital Energy and Orbital Nature of  $[\text{RhCl}_6]^{3-}$ 

MO	Orbital energy (eV) <sup>a)</sup>	Orbital nature <sup>b)</sup>	
Occupied MO			
1t <sub>2g</sub>	-4.08392	M(dπ)+L(pπ)	: Bonding
1a <sub>1g</sub>	-1.84985	M(s)-L(pσ)	: Weakly antibonding
1e <sub>g</sub>	-1.29201	M(dσ)+L(pσ)	: Bonding
1t <sub>1u</sub>	-0.52355	M(p)+L(pσ, pπ)	: Bonding
2t <sub>2g</sub>	0.27701	M(dπ)+L(pπ)	: Bonding
2t <sub>1u</sub>	0.53008	L(pπ)	: Nonbonding, lone pair
3t <sub>1u</sub>	0.90179	M(pπ)+L(pπ)	: Bonding
4t <sub>1u</sub>	1.06370	L(pπ)	: Nonbonding, lone pair
Unoccupied MO			
2e <sub>g</sub>	12.3013	M(dσ)-L(pσ)	: Antibonding
5t <sub>1u</sub>	13.0123	M(pπ)-L(pπ)	: Antibonding
2a <sub>1g</sub>	16.0295	M(dσ)-L(pσ)	: Antibonding

a) Plus values of occupied 2t<sub>2g</sub> to 4t<sub>1u</sub> orbital energies are due to the anion complex  $[\text{RhCl}_6]^{3-}$ . The sign changes minus, when we consider the counter positive ion.

b) M(i) and L(j) denote metal Rh i-type and ligand Cl j-type orbitals, respectively. Plus and minus signs show bonding and antibonding combinations, respectively.

Table 2. Orbital Energy and Orbital Nature of  $[\text{RhCl}_5(\text{H}_2\text{O})]^{2-}$ 

MO	Orbital energy (eV)	Orbital nature <sup>a)</sup>	
Occupied MO			
1a <sub>2</sub>	-7.90905	M(dπ)+L(pπ)	: Bonding
1b <sub>1</sub>	-7.80864	M(dπ)+L(pπ)	: Bonding
1b <sub>2</sub>	-7.38323	M(dπ)+L(pπ)	: Bonding
1a <sub>1</sub>	-5.33130	M(dσ)+L(pσ)	: Bonding
2a <sub>1</sub>	-5.01401	M(dσ)+L(pσ)	: Bonding
3a <sub>1</sub>	-4.10977	M(dπ)+L(pπ)	: Bonding
2b <sub>1</sub>	-3.96582	M(dπ)+L(pπ)	: Bonding
2b <sub>2</sub>	-3.90323	M(dπ)+L(pπ)	: Bonding
2a <sub>2</sub>	-3.36880	M(dπ)+L(pπ)	: Bonding
3b <sub>1</sub>	-3.23682	M(dπ)+L(pπ)	: Bonding
4a <sub>1</sub>	-3.19030	L(pπ)	: Nonbonding, lone pair
3b <sub>2</sub>	-3.10267	M(dπ)+L(pπ)	: Bonding
5a <sub>1</sub>	-3.03273	M(pπ)+L(pπ)	: Bonding
4b <sub>1</sub>	-2.81314	L(pπ)	: Nonbonding, lone pair
4b <sub>2</sub>	-2.81205	L(pπ)	: Nonbonding, lone pair
3a <sub>2</sub>	-2.55027	L(pπ)	: Nonbonding, lone pair
5b <sub>1</sub>	-2.33258	L(pπ)	: Nonbonding, lone pair
5b <sub>2</sub>	-2.28686	L(pπ)	: Nonbonding, lone pair
Unoccupied MO			
6a <sub>1</sub>	8.18362	M(pσ)-L(pσ)	: σ Antibonding
7a <sub>1</sub>	8.39668	M(dσ)-L(pσ)	: σ Antibonding
8a <sub>1</sub>	8.92894	M(dσ)-L(pσ)	: σ Antibonding
6b <sub>1</sub>	9.60815	M(pπ)-L(pπ)	: π Antibonding
6b <sub>2</sub>	9.78448	M(pπ)-L(pπ)	: π Antibonding

a) M(i) and L(j) denote valence i- and j-type orbitals on metal Rh and ligand Cl atoms or ligand O atom of H<sub>2</sub>O molecule, respectively. Plus and minus signs show bonding and antibonding combinations, respectively.

semblance states, since the degenerate was removed owing to symmetry change from  $O_h$   $[\text{RhCl}_6]^{3-}$  to  $C_{2v}$   $[\text{RhCl}_5(\text{H}_2\text{O})]^{2-}$  (see Table 4).

Let us consider the mechanism of the photochemical reactions in the forbidden d-d excited states of the Rh(III) chloroaqua complexes from Rh(dπ)+Ligand-(pπ) bonding MOs to Rh(dσ)-Ligand(pσ) antibonding

MOs. The excitations increase the electron populations in the antibonding MOs, making easier the breaking of the Rh-Ligand bond (Rh-Cl and Rh-OH<sub>2</sub>), since the excitations weaken the Rh-ligand bonds.

**C. Desensitization Produced by Adding Rh-(III) Chloroaqua Complexes on AgCl Grain.** It is interesting to discover why the desensitization of the

Table 3. Active Space, Hartree-Fock Energy and Correlation Energies for the Ground States of Rhodium Chloroaqua Complexes

Rh(III) complex	Hartree-Fock		Correlated		
	Dimension	Energy (a.u.)	Active space (occ×vac)	Energy (SAC)	Correlation energy (a.u.)
[RhCl <sub>6</sub> ] <sup>3-</sup>	75	-110.4607	36 MOs (21×15)	-110.5881	-0.1274
[RhCl <sub>5</sub> (H <sub>2</sub> O)] <sup>2-</sup>	81	-171.9012	41 MOs (26×15)	-172.0155	-0.1143

Table 4. Transition Energies for the Singlet Excited States of Rh(III) Chloroaqua Complexes

Rh(III) complex state	Main configurations	Transition energy	
		Calcd	Obsd
eV			
[RhCl <sub>6</sub> ] <sup>3-</sup>			
<sup>1</sup> T <sub>1g</sub>	1t <sub>2g</sub> →2e <sub>g</sub> ; 2t <sub>2g</sub> ⇒2e <sub>g</sub>	1.97	2.39 (518 nm)
<sup>1</sup> T <sub>2g</sub>	1t <sub>2g</sub> ⇒2e <sub>g</sub> ; 2t <sub>2g</sub> →2e <sub>g</sub>	3.01	3.01 (411 nm)
[RhCl <sub>5</sub> (H <sub>2</sub> O)] <sup>2-</sup>			
(1A <sub>2</sub> , 1B <sub>1</sub> , 1B <sub>2</sub> )		2.33 <sup>a)</sup>	2.44 (506 nm)
1A <sub>2</sub>	1a <sub>2</sub> →7a <sub>1</sub> , 8a <sub>1</sub> ; 2a <sub>2</sub> ⇒7a <sub>1</sub> , 8a <sub>1</sub>	2.36	
1B <sub>1</sub>	1b <sub>1</sub> →7a <sub>1</sub> , 8a <sub>1</sub> ; 3b <sub>1</sub> ⇒7a <sub>1</sub> , 8a <sub>1</sub>	2.29	
1B <sub>2</sub>	1b <sub>2</sub> →7a <sub>1</sub> , 8a <sub>1</sub> ; 3b <sub>2</sub> ⇒7a <sub>1</sub> , 8a <sub>1</sub>	2.33	
(2A <sub>2</sub> , 2B <sub>1</sub> , 2B <sub>2</sub> )		3.23 <sup>a)</sup>	3.08 (402 nm)
2A <sub>2</sub>	1a <sub>2</sub> ⇒7a <sub>1</sub> , 8a <sub>1</sub> ; 2a <sub>2</sub> →7a <sub>1</sub> , 8a <sub>1</sub>	3.16	
2B <sub>1</sub>	1b <sub>1</sub> ⇒7a <sub>1</sub> , 8a <sub>1</sub> ; 3b <sub>1</sub> →7a <sub>1</sub> , 8a <sub>1</sub>	3.16	
2B <sub>2</sub>	1b <sub>2</sub> ⇒7a <sub>1</sub> , 8a <sub>1</sub> ; 3b <sub>2</sub> →7a <sub>1</sub> , 8a <sub>1</sub>	3.36	

a) Values averaged over the three transition energies. Notations: ⇒ and → show dominant and small contributions, respectively.

AgCl photographic emulsions occurs by an addition of a small amount (ppm) of [RhCl<sub>6-n</sub>(H<sub>2</sub>O)<sub>n</sub>]<sup>n-3</sup> (n=0, 1, 2) complexes. We attribute this desensitization phenomenon to be due to the depression of the latent image formation based on the following assumptions:

1. Decrease of an interstitial Ag<sup>+</sup> due to an incorporation of the Rh(III) chloroaqua complex in the formation of the AgCl crystal grain.
2. Deep electron trapping<sup>19,20)</sup> on the Rh(III) complex chemisorbed on or incorporated in the AgCl host lattice.

The latter assumption is generally accepted to interpret the desensitization effect of the Rh-dopant in the AgCl emulsions. We here consider the first assumption, to explain the relative sensitivity increase in the cubic AgCl crystal emulsions containing the chloroaqua rhodium complex compared with a standard emulsion containing [RhCl<sub>6</sub>]<sup>3-</sup> alone.

Let us consider how the [RhCl<sub>6-n</sub>(H<sub>2</sub>O)]<sup>n-3</sup> (n=0, 1, 2) complex cause a decrease of interstitial Ag<sup>+</sup> in the AgCl crystal.

[RhCl<sub>6</sub>]<sup>3-</sup> is incorporated easily in the AgCl lattice, since the Rh(III) chloroaqua and [AgCl<sub>6</sub>]<sup>5-</sup> complexes have the same O<sub>h</sub> symmetry and the bond length is close to each other, Rh-Cl, 2.50 Å and Ag-Cl, 2.78 Å, and since the valence of [RhCl<sub>6</sub>]<sup>3-</sup> are distributed equally along each axis in the AgCl lattice. Thus, the generation of the interstitial Ag<sup>+</sup> in the lattice is decreased by the presence of the Rh(III) complexes.

The [RhCl<sub>5</sub>(H<sub>2</sub>O)]<sup>2-</sup> and [RhCl<sub>4</sub>(H<sub>2</sub>O)<sub>2</sub>]<sup>-</sup> complexes are also easily incorporated in the AgCl crystal lattice, because the symmetries are close to O<sub>h</sub> and the size of the complex is almost as large as [RhCl<sub>6</sub>]<sup>3-</sup>. However, the H<sub>2</sub>O ligand of the Rh chloroaqua complex inside of the AgCl crystal may be replaced by Cl<sup>-</sup> because of the bond strength orders; Ag-Cl ≫ Ag-OH<sub>2</sub> and Rh-Cl < Rh-OH<sub>2</sub>. However, on the surface, the aqua complex can exist. Then, in [RhCl<sub>5</sub>(H<sub>2</sub>O)]<sup>2-</sup>, the charge along the H<sub>2</sub>O-Rh-Cl axis is one valency larger than the other two Cl-Rh-Cl axes, and on [RhCl<sub>4</sub>(H<sub>2</sub>O)<sub>2</sub>]<sup>-</sup>, the charge along the two H<sub>2</sub>O-Rh-Cl axes is one valency larger than the other axis. Thus, according to the charge neutralization principle, the interstitial Ag<sup>+</sup> is produced to balance the charge along these axes.

## Conclusion

We have applied the SAC-CI method to the calculations of the electronic structures and the transition energies of two Rh complexes, [RhCl<sub>6</sub>]<sup>3-</sup> and [RhCl<sub>5</sub>(H<sub>2</sub>O)]<sup>2-</sup>. We have given the HF configurations of the ground states of the Rh(III) complexes and the orbital natures, and the main configurations of the excited states and the calculated transition energies. The theoretical two transition energies of the Rh(III) complexes are in good accordance with the maximum peaks of the visible absorption spectra in aqueous solution. The peaks were assigned to the (<sup>1</sup>T<sub>1g</sub>; <sup>1</sup>T<sub>2g</sub>) and mixed-

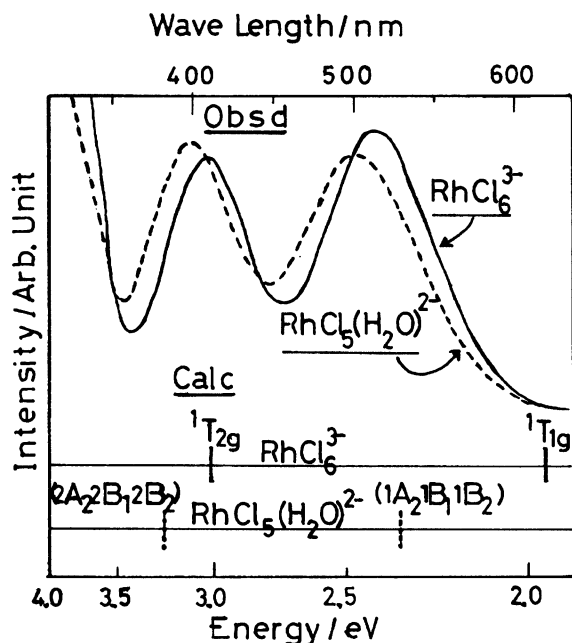


Fig. 1. Electron absorption spectra of  $[\text{RhCl}_6]^{3-}$  and  $[\text{RhCl}_5(\text{H}_2\text{O})]^{2-}$  complexes with the calculated marks using the ab initio SAC/SAC-CI method. The upper spectra show observed absorption ones of the Rh(III) complexes. The lower marks indicate the calculated two peaks for each Rh(III) complex.

( $1\text{B}_1$ ,  $1\text{A}_2$ ,  $1\text{B}_2$ ;  $2\text{B}_1$ ,  $2\text{A}_2$ ,  $2\text{B}_2$ ) states for  $[\text{RhCl}_6]^{3-}$  and  $[\text{RhCl}_5(\text{H}_2\text{O})]^{2-}$  complexes, respectively. These are the essentially forbidden d-d transitions and are due to the excitations from the Rh( $d\pi$ )+Ligand( $p\pi$ ) bonding MOs to the Rh( $d\sigma$ )-Ligand( $p\sigma$ ) antibonding MOs. This excitation weakens the metal-ligand bonds. We have finally described the mechanism of the desensitization due to the decrease of an interstitial  $\text{Ag}^+$  produced by addition Rh(III) chloroqua complexes to the AgCl grain in the emulsion.

Although we cannot ignore the solvent effects in the case where the analysis of the transition energies of the visible absorption spectra of these Rh-complexes in solution is discussed in more detail, we know that the transition states of the metal complexes in solution can have been identified in terms of the calculation results in gas phase using the SAC/SAC-CI method.<sup>12)</sup> The result in this study was shown from such a viewpoint. We will consider the solvent effects on the ground and ex-

cited states of metal-complexes in solution as a subject in the future.

#### References

- 1) M. T. Beck, P. Kiss, T. Szalay, E. C. Porzolt, and G. Bazsa, *J. Signal Am.*, **4**, 131 (1976).
- 2) K. Endo and M. Saikawa, *J. Photogr. Sci.*, **38**, 210 (1990).
- 3) W. Robb and G. M. Harris, *J. Am. Chem. Soc.*, **87**, 4472 (1965).
- 4) K. Swaminathan and G. M. Harris, *J. Am. Chem. Soc.*, **88**, 4411 (1966).
- 5) W. Robb and M. M. De V. Steyn, *Inorg. Chem.*, **6**, 616 (1967).
- 6) M. J. Pavelich and G. M. Harris, *Inorg. Chem.*, **12**, 423 (1973).
- 7) D. A. Palmer and G. M. Harris, *Inorg. Chem.*, **14**, 1316 (1975).
- 8) B. R. James and M. Kastner, *Can. J. Chem.*, **50**, 1708 (1972).
- 9) H. Nakatsuji and K. Hirao, *J. Chem. Phys.*, **68**, 2053 (1978).
- 10) H. Nakatsuji, *Chem. Phys. Lett.*, **59**, 362 (1978); **67**, 329 (1979).
- 11) H. Nakatsuji, *J. Chem. Phys.*, **80**, 3703 (1984); *Chem. Phys.*, **75**, 425 (1983).
- 12) H. Nakatsuji, *Acta Chim. Acad. Sci. Hung.*, **129**, 719 (1992).
- 13) P. H. Hay and W. R. Wadt, *J. Chem. Phys.*, **82**, 270 (1985).
- 14) W. R. Wadt and P. H. Hay, *J. Chem. Phys.*, **82**, 284 (1985).
- 15) T. H. Dunning, Jr., *J. Chem. Phys.*, **53**, 2823 (1970).
- 16) R. B. Brooks, P. Saxe, W. D. Laidig, and M. Dupuis, "Program System GAMESS, Program Library No. 481," Computer Center of the Institute for Molecular Science, 1981.
- 17) Y. Tanabe and S. Sugano, *J. Phys. Soc. Jpn.*, **9**, 753, 766 (1954).
- 18) A. B. P. Lever, "Inorganic Electronic Spectroscopy," Elsevier Publishing Co., Amsterdam (1968); D. Cozzi and F. Pantani, *J. Inorg. Nucl. Chem.*, **8**, 385 (1958); W. C. Wolsey, C. A. Reynolds, and J. Kleinberg, *Inorg. Chem.*, **2**, 463 (1963).
- 19) R. S. Eachus and R. E. Graves, *J. Chem. Phys.*, **61**, 2860 (1974).
- 20) T. Tani and M. Sato, *Sci. Publ. Fuji Photo Film Co., Ltd.*, **19**, 66 (1972); **20**, 84 (1973).